ON THE EXISTENCE OF INDEPENDENT SYMBOLIC DYNAMICS FOR WEAK COUPLING OF CHAOTIC SYSTEMS

Zbigniew Galias

Department of Electrical Engineering, University of Mining and Metallurgy, Kraków, Poland
galias@zet.agh.edu.pl

Abstract— In this paper we study behavior of coupled continuous–time chaotic systems by means of independent symbolic dynamics. First we consider the perturbed chaotic system and estimate the maximum perturbation range for which the symbolic dynamics survives. If the coupling is small enough then the perturbation introduced by the coupling does not exceed the maximum range and there exists independent symbolic dynamics for every coupled subsystem. As an example we consider coupled Chua circuits. We compute the value of the coupling strength for which the symbolic dynamics in every subsystem is not destroyed.

I. INTRODUCTION

Since the first observations of coupled chaotic systems displaying identical oscillations [1, 2, 3] there has been a considerable interest in using the concept of synchronization of chaos to develop spread spectrum communication systems. For the applications of synchronized chaos it is very important to develop methods for studying the synchronization phenomena.

Recently we have introduced a method for investigating of coupled chaotic systems based on the existence of robust symbolic dynamics [4]. The method consists of two steps. First for every subsystem we find the perturbation range for which we can verify that the symbolic dynamics is not destroyed. In the second step we check that the perturbation introduced by the coupling is smaller than the maximum allowable perturbation. If this condition holds for each subsystem then the independent symbolic dynamics in every subsystem exists. In consequence, the subsystems are not uniformly synchronized in the sense that there exist trajectories of the whole system realizing arbitrary allowable sequences in every subsystem.

Previously we have applied this method for a discrete-time system, namely the Hénon map. In this paper we adapt the method for continuous–time systems. The extension is not straightforward and is discussed in detail in the following sections.

In section 2 we recall the results on the existence of symbolic dynamics for the Chua's system. In section 3 we address the problem of proving the existence of symbolic dynamics for perturbed continuous–time chaotic systems. We describe the procedure which is used for computation of the maximum perturbation range which does not destroy the symbolic dynamics. In section 4 we study behavior of coupled Chua's circuits by means of independent symbolic dynamics. We estimate the coupling value for which the systems are not synchronized due to the existence of independent symbolic dynamics.

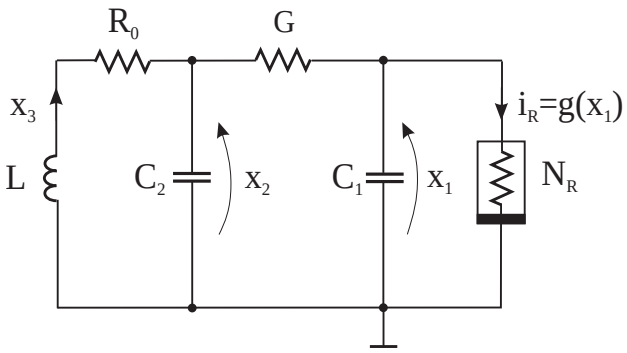

Figure 1: Chua's circuit.

II. SYMBOLIC DYNAMICS FOR CHUA'S CIRCUIT

In this section we recall the results on the existence of symbolic dynamics for a three–dimensional nonlinear electronic circuit shown in Fig. 1. Its dynamics is described by the following state equation:

$$\begin{aligned} C_1\dot{x_1} &= G(x_2-x_1)-g(x_1), \\ C_2\dot{x_2} &= G(x_1-x_2)+x_3, \\ L\dot{x_3} &= -x_2-R_0x_3, \end{aligned} \tag{1a}$$

where $g(\cdot)$ is a three-segment piecewise-linear characteristics (compare Fig. 2):

$$g(x)=G_bx+0.5(G_a-G_b)(|x+1|-|x-1|). \tag{1b}$$

We use parameter values ($C_1=1$, $C_2=9.3515$, $L=0.06913$, $R=0.33065$, $G_a=-3.4429$, $G_b=-2.1849$, $R_0=0.00036$) for which the famous double-scroll chaotic attractor is observed.

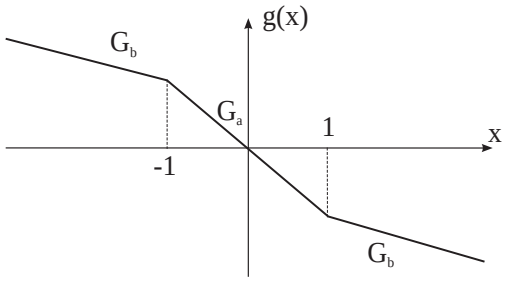

Figure 2: Characteristics of nonlinear resistor.

The symbolic dynamics corresponding to the deformed horseshoe is observed for the Poincaré map P defined by the plane $V_+ = \{ x = (x_1, x_2, x_3) \in \mathbb{R}^3 : x_1 = 1 \}$. On this plane we choose eight points $A_1, \ldots, A_8$ defining quadrangles $N_0 = A_5A_6A_7A_8$ and $N_1 = A_1A_2A_3A_4$. The "horizontal" sides of N_0 and N_1 are defined as $N_{1U} = \overline{A_1A_2}$, $N_{1D} = \overline{A_3A_4}$, $N_{0U} = \overline{A_5A_6}$, $N_{0D} = \overline{A_7A_8}$. Parallel lines A_1A_4 and A_2A_3 define the stripe S. The sets M_0, M_+ and M_- are defined as parts of the stripe S (compare Fig. 3). For exact definitions of points $A_1, \ldots, A_8$ and sets N_0, N_1, M_-, M_0 and M_+ see [5].

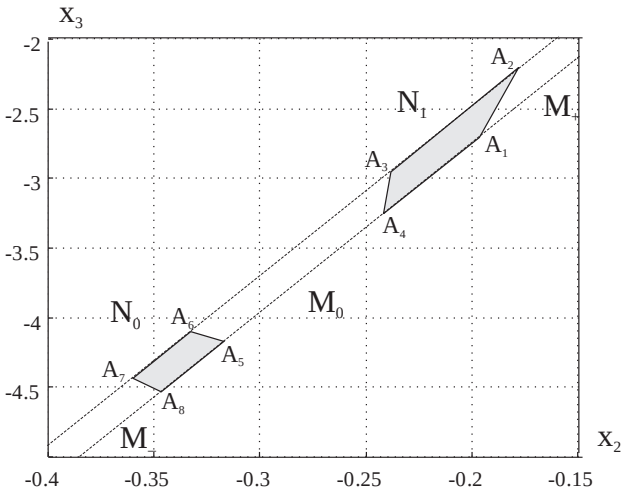

Figure 3: Sets N_0, N_1, M_-, M_0 and M_+ on the transversal plane.

Let Σ_G be the golden subshift of a finite type

$$\Sigma_G = \{(a_0, a_1, \ldots) \in \Sigma_2 \colon (a_i, a_{i+1}) \neq (1,1) \text{ for } i \geq 0\}.$$

where Σ_2 is the space of all (one-sided) sequences with symbols in the set $\{0, 1\}$. By $\sigma : \Sigma_2 \mapsto \Sigma_2$ we denote the shift map defined by $\sigma(s)_i = s_{i+1}$ for $i \geq 0$.

In order to prove that the symbolic dynamics corresponding to the golden subshift is embedded in P we use the following theorem.

Theorem 1. *If P is continuous on $N_0 \cup N_1$, $P(N_0), P(N_1) \subset \operatorname{int} S$, horizontal edges of N_0, N_1 are mapped by P in such way that one of the sets $P(N_{0D})$, $P(N_{0U})$ is enclosed in M_+, while the second one is enclosed in M_-, one of the sets $P(N_{1D})$, $P(N_{1U})$ is enclosed in M_-, while the second one is enclosed in $M_0 \cup N_1 \cup M_+$ then there exists continuous surjective map $\pi \colon \operatorname{Inv}(N_0 \cup N_1, P) \mapsto \Sigma_G$, such that*

$$\pi \circ P = \sigma \circ \pi,$$

where $\operatorname{Inv}(N_0 \cup N_1, P)$ denotes the invariant part of $N_0 \cup N_1$ under P. The preimage of any periodic sequence from Σ_G contains periodic points of P.

Using computer interval arithmetic we have shown that the assumptions of the above theorem are fulfilled [5]. We have proved that there exists a continuous Poincaré map defined on $N_0 \cup N_1$, the images $P(N_{0L})$, $P(N_{0R})$, $P(N_{1L})$, $P(N_{1R})$ of "vertical" edges of quadrangles N_0, N_1 lie inside stripe P, and that the images of "horizontal" edges of N_0, N_1 fulfills the following conditions: $P(N_{0D}) \subset P_{0D} \subset M_+$, $P(N_{0U}) \subset P_{0U} \subset M_-$, $P(N_{1D}) \subset P_{1D} \subset M_-$, $P(N_{1U}) \subset P_{1U} \subset M_0$ (compare Fig. 4).

It follows that the symbolic dynamics corresponding to the golden subshift is embedded in P.

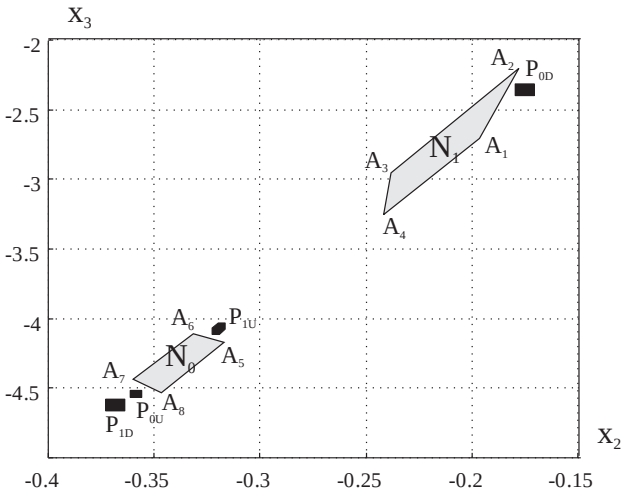

Figure 4: Images of edges of N_0, N_1 under the Poincaré map.

III. SYMBOLIC DYNAMICS FOR THE PERTURBED SYSTEM

In this section we show how to prove the existence of symbolic dynamics for a Poincaré map P of a perturbed continuous–time system. The main difference with the case of maps is that the perturbation is not added directly to the Poincaré map but modifies the vector field and in this way influences P.

We consider the perturbed Chua's system

$$\begin{aligned} \dot{x_1} &= G(x_2 - x_1)/C_1 - g(x_1)/C_1 + e_1, \\ \dot{x_2} &= G(x_1 - x_2)/C_2 + x_3/C_2 + e_2, \\ \dot{x_3} &= -x_2/L - R_0 x_3/L + e_3, \end{aligned} \tag{2}$$

where $(e_1, e_2, e_3) = (e_1(t), e_2(t), e_3(t))$ is the perturbation. We assume that the perturbation is bounded, i.e. $||e|| \leq \varepsilon$. We want to find ε for which the symbolic dynamics survives. In [5] we have used the piecewise linearity of the Chua's system to prove the assumptions of Theorem 1. In case of perturbed system we cannot proceed in this way due to the existence of perturbation term. Instead we have to integrate the system equation using a computer integration procedure (compare [6]) and take into account errors coming from the perturbation.

First let us describe the procedure for computation of the image of a rectangle under Poincaré map. During this procedure the system (3) is integrated using the combination of the fourth-order Taylor integration method and techniques based on differential inequalities [7]. We rigorously compute the errors caused by omitting higher order terms in the intergration procedure. All the operations are performed in 'interval arithmetic' to obtain rigorous errors for elementary operations. In every integration step we compute the image of the Euclidean ball $\mathrm{B}(C, \varrho)$ after time h. C is the point interval and ϱ is the radius of the considered ball. First we compute the image of the center interval C using the fourth-order Taylor integration method with rigorous estimation of error. Then using the following theorem we compute how the ball with radius ϱ changes its size during evolution after time h.

Theorem 2 (theorem 10.6 from [7]). *Let $y(t)$ be a solution and $v(t)$ be an approximate solution of the system of differential equations $x' = f(x)$. Suppose that we have following estimates:*
(a) $||v(t_0) - y(t_0)|| \leq \varrho$,
(b) $||v'(t) - f(v(t))|| \leq \varepsilon$,
(c) *The logarithmic norm $m(f'(\cdot)) \leq L$ on the convex set containing trajectories $\{v(t) : t \in [t_0, t_1]\}$ and $\{y(t) : t \in [t_0, t_1]\}$.*
Then for $t \in [t_0, t_1]$ we have the estimate

$$||y(t) - v(t)|| \leq \varrho \mathrm{e}^{L(t-t_0)} + \frac{\varepsilon}{L}\left(\mathrm{e}^{L(t-t_0)} - 1\right). \tag{3}$$

Let us recall that the Logarithmic norm [7] of matrix Q is defined by

$$m(Q) := \lim_{h \to 0, h > 0} \frac{||I + hQ|| - 1}{h}.$$

For the Euclidean norm on the right side of the above equation the logarithmic norm of Q can be computed as the largest eigenvalue of the matrix $\frac{1}{2}(Q^T + Q)$.

The radius of the ball after time h is computed using right hand side of inequality (3). Using this formula we estimate errors coming from two sources. Condition (a) measures the error in initial conditions (the size of the initial ball is ϱ). Condition (b) measures the extent to which function $v(t)$ does not satisfy the imposed differential equation. In the case of perturbed system we have

$$v' = f(v) + e,$$

where e is the perturbation. Obviously $||e|| = ||v' - f(v)||$ and hence the condition (b) means that the maximum amplitude of the perturbation is smaller than ε.

L is the upper bound of the logarithmic norm of the matrix f' over the set containing all the trajectories starting from the ball $\mathrm{B}(C, \varrho)$ after time $t \in [0, h]$.

During the procedure for the whole Poincaré map we perform subsequent integration steps obtaining images of the initial rectangle after $h, 2h, \ldots$. This is continued until the intersection with the transversal plane is finished. In this way we obtain values t_1 and t_2, where t_1 corresponds to the last integration step for which trajectory lies before transversal plane and t_2 corresponds to the first integration step for which trajectory lies completely after transversal plane. Then we compute an interval vector containing trajectories starting from the initial rectangle after time $[t_1, t_2]$. The image of the initial rectangle under Poincaré map is contained in the projection of this interval vector to the transversal plane.

Once we have the procedure for computation of the image of a rectangle under Poincaré map of the perturbed system we can check the assumptions of Theorem 1. We proceed in the following way. First we choose ε. Then we cover the region under investigation by rectangles and compute their images under Poincaré map of the perturbed system using the procedure described above. Finally we check if the assumptions of the existence theorem hold.

In our study we have chosen $\varepsilon = 10^{-7}$ and checked that the assumptions of Theorem 1 for the perturbed Chua's system are fulfilled. The perturbation for which we were able to prove the existence of symbolic dynamics is very small.

In order to estimate the real value of the maximum allowed perturbation we integrate the Chua system using particular values of perturbation. We assume that $e_2 = e_3 = 0$. We have checked that for $e_1 = 0.0008$ and for $e_1 = -0.0007$ the symbolic dynamics exists. For larger perturbation one cannot prove the existence theorem. For $e_1 = 0.0009$ the image of N_{0D} touches N_1 and the condition $P(N_{0D}) \subset M_+$ is not true. For $e_1 = -0.0008$ the image of N_{0U} touches N_0 (the condition $P(N_{0U}) \subset M_-$ does not hold) and the image $P(N_{0D})$ breaks in two parts (the Poincaré map is not continuous on N_0).

This is indication that the symbolic dynamics survives for perturbation $|e_1| \leq 0.0007$. One can easily see that symbolic dynamics for the Chua's circuit is not robust, i.e. it can be destroyed by very small perturbation.

IV. COUPLED CIRCUITS

In this section we analyze the behavior of coupled Chua's circuits using the results from the previous section. Two Chua's circuits are coupled bi-directionally by means of conductance G_1 between the capacitors C_1 (compare Fig. 5).

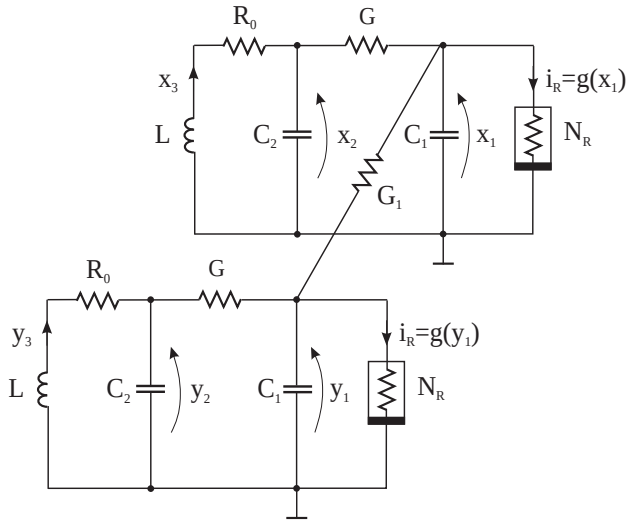

Figure 5: Coupled Chua's circuits

The dynamics of the coupled system is described by the following equations:

$$\begin{aligned} C_1\dot{x}_1 &= G(x_2 - x_1) - g(x_1) + G_1(y_1 - x_1), \\ C_2\dot{x}_2 &= G(x_1 - x_2) + x_3, \\ L\dot{x}_3 &= -x_2 - R_0 x_3, \\ C_1\dot{y}_1 &= G(y_2 - y_1) - g(y_1) + G_1(x_1 - y_1), \\ C_2\dot{y}_2 &= G(y_1 - y_2) + y_3, \\ L\dot{y}_3 &= -y_2 - R_0 y_3. \end{aligned} \tag{4}$$

In order to check whether the symbolic dynamics survives we have to check that the perturbation introduced by the coupling is small enough. The error term is given by

$$e_1 = G_1(y_1 - x_1)/C_1; \tag{5}$$

We have to find G_1 for which $|e_1| \leq e_{1\max}$, where $e_{1\max}$ is the maximum perturbation for which the symbolic dynamics survives. As we investigate the existence of symbolic dynamics, we know that $x_1, y_1 \in [0, 2.3]$. Hence $(y_1 - x_1)/C_1 \in [-2.3, 2.3]$. Finally for $G_1 \leq e_{1\max}/2.3$ the condition $|e_1| \leq e_{1\max}$ holds.

In the previous section we estimated that for $e_{1\max} = 0.0007$ the eprturbed Chua's system displays the symbolic dynamics and hence there is strong indication that for $G_1 < 0.0003$ there exist independent symbolic dynamics in coupled Chua's circuits.

V. CONCLUSIONS

In this paper we have adressed the problem of robustness of symbolic dynamics for continuous–time chaotic systems. We have shown that the symbolic dynamics embedded in the Poincaré map is not destroyed if the perturbation is small enough. We have developed a method for computing the perturbation range which does not destroy the symbolic dynamics. For the Chua's circuits using computer interval arithmetic we have found sufficient conditions for the perturbation, which does not destroy the symbolic dynamics. We have also estimated the real value of perturbation for which the proof cannot be carried out. For coupled Chua's circuits we have computed the value of coupling conductance for which there exist independent symbolic dynamics in coupled systems.

Acknowledgments

This work was supported by Polish Committee of Scientific Research KBN, grant no. 2/P03A/021/15. The author would like to thank Dr. P. Zgliczyński for discussions.

References

[1] H. Fujisaka and T. Yamada, "Stability theory of synchronized motion in coupled–oscillator systems," *Prog. Theor Phys.*, vol. 69, no. 1, pp. 32–47, 1983.

[2] V.S. Afraimovich, N.N. Verichev, and M.I. Rabinovich, "Stochastic synchronization of oscillations in dissipative systems," *Izv. VUZ Radiofiz.*, vol. 29, pp. 795–803, 1986.

[3] L. Pecora and T. Carroll, "Driving systems with chaotic signals," *Phys. Rev. A*, vol. 44, no. 4, pp. 2374–2383, 1991.

[4] Z. Galias, "Robustness of symbolic dynamics and synchronization properties," accepted for publication in Int. J. Bifurcation and Chaos, 1999.

[5] Z. Galias, "Positive topological entropy of Chua's circuit: A computer assisted proof," *Int. J. Bifurcation and Chaos*, vol. 7, no. 2, pp. 331–349, 1997.

[6] Z. Galias and P. Zgliczyński, "Computer assisted proof of chaos in the Lorenz equations," *Physica D*, vol. 115, pp. 165–188, 1998.

[7] E. Hairer, S.P. Nørsett, and G. Wanner, *Solving ordinary differential equations. I. Nonstiff problems*, Springer–Verlag.